The Astrophysical Journal, 650: L107–L110, 2006 October 20

ACS PHOTOMETRY OF THE REMOTE M31 GLOBULAR CLUSTER B514[1]

S. Galleti,[2] L. Federici,[2] M. Bellazzini,[2] A. Buzzoni,[2] and F. Fusi Pecci[2]

Received 2006 July 13; accepted 2006 September 5; published 2006 October 2

ABSTRACT

We present deep F606W, F814W ACS photometry of the recently discovered globular cluster B514, the outermost known globular in the M31 galaxy. The cluster appears quite extended, and member stars are unequivocally identified out to ~200 pc from the center. The color-magnitude diagram reveals a steep red giant branch (RGB), and a horizontal branch extending blueward of the instability strip, indicating that B514 is a classical old metal-poor globular cluster. The RGB locus and the position of the RGB bump are both consistent with a metallicity [Fe/H] ~ -1.8, in excellent agreement with spectroscopic estimates. A preliminary estimate of the integrated absolute V magnitude ($M_V \lesssim -9.1$) suggests that B514 is among the brightest globulars of M31.

Subject headings: galaxies: individual (M31) — globular clusters: individual (B514) — stars: abundances — stars: Population II

1. INTRODUCTION

Stars and stellar systems orbiting the most external regions of their parent galaxy are crucial tracers of the mass distribution and the formation history of the parent galaxy as a whole. For example, it is well known that substructures related to accretion events are best preserved in the outskirts of a galactic halo (see, e.g., Bullock & Johnston 2004 and references therein). In this context globular clusters may serve as excellent tracers of substructures in the outer region of their parent galaxy. For instance, Bellazzini et al. (2003) were able to identify the accretion signature of the Sagittarius dwarf galaxy among the globular clusters in the outer halo of the Milky Way.

As large substructures are also identified in the nearby spiral galaxy M31 (Ibata et al. 2001) it becomes increasingly important to have a complete census of the cluster population in the galaxy outskirts—still lacking to date (see Galleti et al. 2005, 2006)—as well as to collect information about cluster ages, metal content, kinematics, etc. Several groups are currently working on this line (Huxor et al. 2004; Bates et al. 2004), including ourselves (see Galleti et al. 2004, 2005, 2006). In particular, in Galleti et al. (2005, hereafter G05) we reported on the discovery of the outermost known cluster of M31, B514 located at a projected distance of $R_p \simeq 55$ kpc from the center of M31, not far from the galaxy major axis. The integrated photometry and spectroscopy indicates that B514 is likely an old metal-poor globular cluster (G05); however direct imaging, at a spatial resolution sufficient to resolve the system into stars, is the only way to ultimately ascertain the nature of a candidate globular in M31 (see Galleti et al. 2004, 2006).

Here we present the first results of follow-up observations of B514 taken with the Wide Field Camera (WFC) of the Advanced Camera for Surveys (ACS) on board the *Hubble Space Telescope* (*HST*), confirming that the object is a genuine old and metal-poor cluster lying in the remotest region of M31.

2. DATA ANALYSIS

Observations were carried out on 2006 June 10 (program ID GO 10565, PI: S. Galleti). We acquired three images with the F606W filter, for a total exposure time of $t_{\rm exp} = 2412$ s, and three F814W images, for a total exposure time of $t_{\rm exp} = 2418$ s. The ACS WFC camera is a mosaic of two 4096 × 2048 pixel^2 CCDs, with a pixel scale of $0\farcs05$ pixel^{-1}. The pointing was chosen such as to have the cluster placed near the center of one of the ACS WFC CCDs (chip 2), while chip 1 is presumed to sample the stellar population in the field surrounding the cluster. Data reduction has been performed on the individual prereduced images provided by STScI, using the ACS module of DOLPHOT[3] (Dolphin 2000), a point-spread function fitting package specifically devoted to the photometry of *HST* data. The package identifies the sources and performs the photometry on individual frames, also taking into account all the information about image cosmetics and cosmic-ray hits that is attached to the observational material. DOLPHOT provides as output the magnitudes and positions of the detected sources, as well as a number of quality parameters for a suitable sample selection, in view of the actual scientific objective one has in mind. Here we selected all the sources having valid magnitude measurements in both passbands, global quality flag = 1 (i.e., best measured stars), *crowding* parameter <0.3, and $\chi^2 < 1.5$ if F606W < 24.0, and $\chi^2 < 2.5$ for brighter stars (see Dolphin [2000] for details on the parameters). This selection cleans the sample from the vast majority of spurious and/or bad measured sources without significant loss of information. The magnitudes have been reported to the VEGAMAG system following the prescriptions of Sirianni et al. (2005). For reddening corrections, in the following we always adopt $A_{\rm F606} = 2.809E(B-V)$ and $A_{\rm F814} = 1.825E(B-V)$, from Sirianni et al. (2005). These extinction laws are appropriate for a G2 star, but for $E(B-V) \leq 0.1$ they are accurate to within 0.01 mag for a large range of spectral types (from O5 to M0, according to Sirianni et al. 2005).

Figure 1 shows a section of the combined (drizzled) F606W image centered on B514. The exquisite spatial resolution of the ACS WFC clearly resolves the object into stars, revealing a beautiful globular cluster with an extended halo. We were able to obtain useful photometry of individual stars down to a distance of $r \simeq 2\farcs5$ from the cluster center, that we identified at the position of the peak in the light profile at $x_{\rm pixel} = 2084$ and $y_{\rm pixel} = 1021$ on chip 2. In any case the adopted selection criteria excludes from the adopted sample the stars

[1] Based on observations with the NASA/ESA *Hubble Space Telescope*, obtained at the Space Telescope Science Institute (STScI), which is operated by AURA, Inc., under NASA contract NAS 5-26555.

[2] INAF–Osservatorio Astronomico di Bologna, via Ranzani 1, I-40127 Bologna, Italy.

[3] See http://purcell.as.arizona.edu/dolphot/.

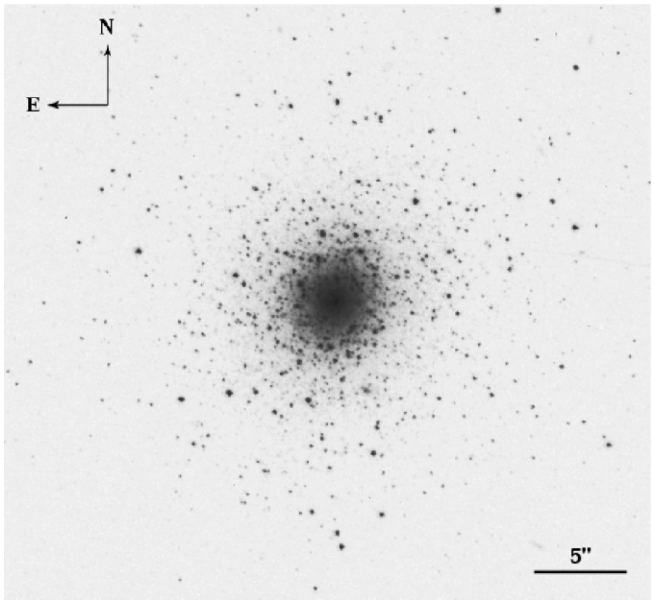

FIG. 1.—B606W image of B514.

located in the most crowded region of the cluster. In particular, the adopted sample contains no stars with $r \leq 2\farcs5$ and only 44 bright star (over a total sample of 1562 stars in chip 1) having $r \leq 5''$.

3. THE COLOR-MAGNITUDE DIAGRAM OF B514

In Figure 2 we plot the color-magnitude diagrams (CMDs) of different radial annuli around the cluster center in chip 2 (Figs. 2*a*, 2*b*, and 2*c*) and of all the stars detected in chip 1 (Fig. 2*d*). Most of the cluster stars are obviously in the inner-

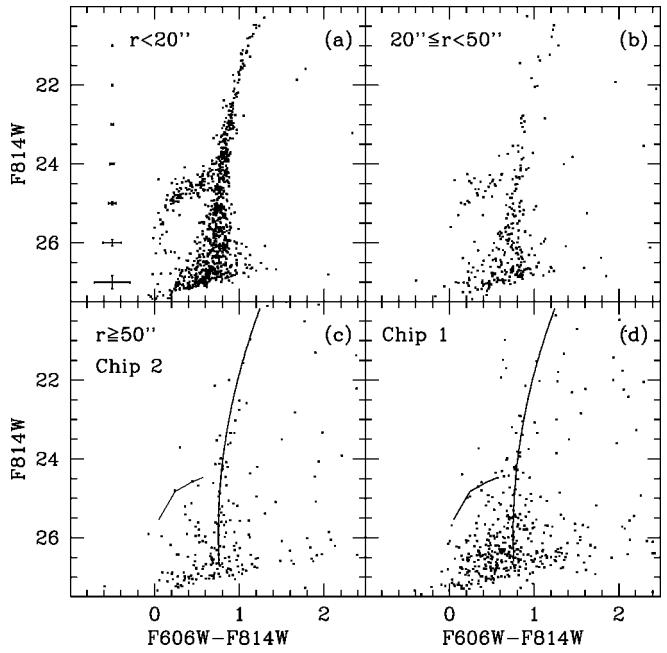

FIG. 2.—(*a*–*c*) CMDs of different radial annuli centered on the center of the cluster. The considered annuli sample the following fraction of the area of chip 2, approximately (*a*) 6%, (*b*) 33%, and (*c*) 60%, respectively. The fiducial ridge lines of the cluster are superposed to the CMD in panel *c*. (*d*) CMD of all the stars in chip 1 (sampling the field population) with the cluster fiducial ridge lines superposed (solid lines).

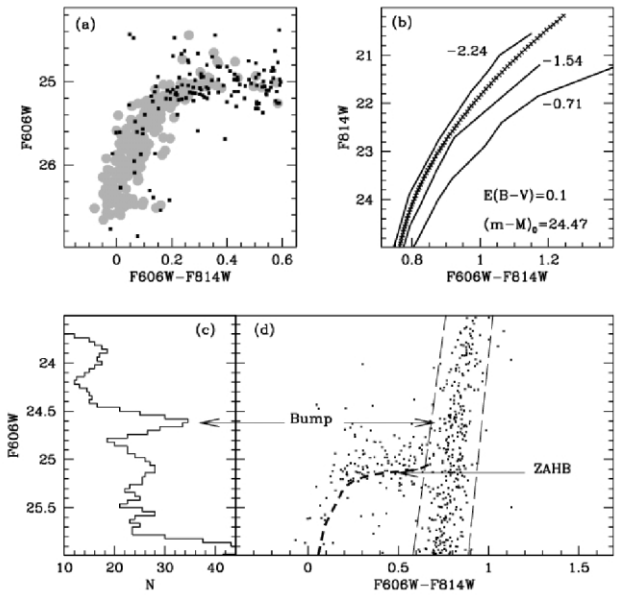

FIG. 3.—(*a*) Comparison between the (*blue*) HBs of B514 (*black dots*) and M92 (*gray circles*), obtained assuming $E(B-V) = 0.1$ and $(m-M)_0 = 24.47$ for B514, similar to G05. (*b*) Comparison between the RGB ridge line of B514 (*crosses*) and those of template Galactic clusters (*solid lines*) from Brown et al. (2005). From left to right the fiducials are M92, NGC 6752, and 47 Tuc. The corresponding metallicities are labeled on the plot. (*c*) Luminosity function of the RGB of B514 presented as a smoothed histogram with step of 0.04 mag and bin of 0.2 mag. The arrow indicates the position of the RGB bump. (*d*) CMD of B514 with the position of the RGB bump and the ZAHB indicated by arrows. The long-dashed line is the ZAHB model for $Z = 0.0003$ and $Y = 0.245$ by Pietrinferni et al. (2006) in the ACS VEGAMAG photometric system, corrected for the assumed reddening and distance modulus of B514. The dashed lines mark the region of CMD that was used to create the luminosity function in panel *c*.

most region; hence, the diagram of Figure 2*a* shows more clearly the main evolutionary sequences. The CMD is dominated by an extended and very steep red giant branch (RGB) going from F814W ~ 20.5 and F606W − F814W ≃ 1.1 down to the limiting magnitude level at F606W − F814W ≃ 0.9. A small overdensity corresponding to the RGB bump (see below) is discernible at F814W ≃ 23.8. The horizontal branch (HB) appears quite extended in color. A sloped band of stars crossing the sequence at F814W ≃ 24.6 and F606W − F814W ≃ 0.4 has the typical appearance of a population of RR Lyrae stars sampled at random phase, strongly suggesting the presence of a significant number of such variables (see also Fig. 3*a*). The HB is clearly well populated to the blue of the instability strip with a possible hint to the presence of extreme HB stars at F814W > 25.0 and F606W − F814W ~ 0.0. The mere presence of blue HB stars and RR Lyrae indicates that the cluster is probably older then 10 Gyr. The possible presence of HB stars lying to the red of the instability strip needs a more detailed analysis to be considered in the present context. This, as well as other issues, is demanded to a future, more thorough contribution (S. Galleti et al. 2006, in preparation, hereafter Paper II).

The diagram in Figure 2*d* shows that the stellar density in these extreme regions of M31 is so low that the field of view of a single ACS WFC CCD is insufficient to sample the evolved population of the M31 halo; hence, no clear RGB and/or HB

sequence can be identified and the degree of contamination of the cluster CMD should be negligible, at least for F814W $\leq$ 26.0. As a reference, we have overplotted in Figure 2*d* the ridge lines of the RGB and HB of B514, derived as in Ferraro et al. (1999, hereafter F99). Note that the sky area sampled by the CMD of Figures 2*a*, 2*b*, and 2*c* is ~6%, ~33%, and ~60%, respectively, of the area of chip 1 (CMDs of Fig. 2*d*).

Figure 2*b* shows that cluster RGB and HB are clearly visible out to a radius of >20″, corresponding to $\simeq$76 pc at the distance of M31 (assuming $D = 783$ kpc, from McConnachie et al. 2005). A value of $r = 50''$ is the radius of the largest circle centered on the cluster that is completely enclosed within chip 2. In Figure 2*c* we plot chip 2 stars having $r \geq 50''$: the CMD is too sparsely populated here to establish whether cluster stars are found this far from the cluster center. While the detailed analysis of the cluster profile will be presented in Paper II, we already anticipate that a break in the profile is clearly detected around the tidal radius of the cluster (at $r \sim 20''$), suggesting the presence of extratidal stars (Johnston et al. 1999).

3.1. *Distance, Metallicity, and the RGB Bump*

In Figure 3 we present a series of diagrams illustrating our assumptions on distance and reddening, our estimates of the metallicity of B514, and the detection of the RGB bump of the cluster:

Figure 3*a*.—We assume $(m - M)_0 = 24.47$, after McConnachie et al. (2005) and $E(B - V) = 0.1$, similar to G05. To check the consistency of these assumptions we compare the BHB of B514 with that of the metal-poor Galactic globular M92 (NGC 6341). The ACS data for M92 are from the set presented by Brown et al. (2005); here we have reduced and calibrated the shortest exposures in a fully homogeneous way to obtain a comparison with B514 as self-consistent as possible. The reddening and distance modulus of M92 are taken from F99 (cols. [5] and [8], respectively, of their Table 2). The HB morphology of M92 is sufficiently similar to the B514 one to provide a wide overlap in the portion of the BHB that is more suitable to be used as a standard candle, for example, in the range $0.2 \leq$ F606W $-$ F814W ≤ 0.35, where the sequence is nearly horizontal. The diagram clearly show that our assumed distance and reddening provide a very good match between the BHB of the two clusters, fully supporting our choices.

Figure 3*b*.—The RGB ridge line of B514 (already presented in Fig. 2) is compared with the RGB fiducials of the Galactic clusters M92, NGC 6752, and 47 Tucanae, taken from Brown et al. (2005) and corrected for our assumed distance and reddening. The fiducial lines are labeled with their [Fe/H] value in the Zinn (1985) scale, from F99. Reddening and distance moduli of the templates are taken from F99. The RGB of B514 is nicely enclosed between the fiducials at [Fe/H] $= -2.24$ and [Fe/H] $= -1.54$, in good agreement with the spectroscopic estimate of [Fe/H] $= -1.8$ provided by G05.

Figure 3*c*.—The RGB bump is a well-known feature in the luminosity function of the RGB of globular clusters (see F99 for details and references). The bump is clearly identified here as a peak in the LF of the RGB of B514, at F606W $= 24.62 \pm 0.05$. RGB stars were selected in the CMD using a color-magnitude window that follows the RGB ridge line, excluding HB stars and field stars. A RGB bump brighter than the HB level is typical of metal-poor globular clusters.

Figure 3*d*.—A theoretical zero-age HB (ZAHB) sequence (with $Z = 3 \times 10^{-4}$ and $Y = 0.245$) is superposed to the CMD of B514. The sequence is taken from the set by Pietrinferni et al. (2006), transformed to the ACS system by Bedin et al. (2005), and corrected for the reddening and distance modulus assumed above. As expected, the theoretical ZAHB lies at the faint end of the observed HB. We take the ZAHB luminosity at F606W $-$ F814W $= 0.4$ as the fiducial ZAHB level, $\mathrm{F606W_{HB}} = 25.14$. The magnitude difference between the bump and the HB is $\Delta\mathrm{F606W_{HB}^{bump}} = -0.62 \pm 0.1$. We transformed the F606W magnitudes of the bump and the ZAHB into Johnson-Cousins V magnitudes by using the relation

$$V = \mathrm{F606W} + 0.205C^2 + 0.104C + 0.037, \qquad (1)$$

where $C =$ (F606W $-$ F814W), which we have obtained from more than 400 stars in common between our ACS photometry of M92 and the set of secondary photometric standards in M92 by Stetson (2000). From the obtained values, $V_{\mathrm{bump}} = 24.89$ and $V_{\mathrm{HB}} = 25.25$, we compute $\Delta V_{\mathrm{HB}}^{\mathrm{bump}} = -0.36 \pm 0.12$ mag, which can be used as input for the relations by F99 between $\Delta V_{\mathrm{HB}}^{\mathrm{bump}}$ and [Fe/H], calibrated on Galactic globulars, to obtain an independent estimate of the metallicity from the Bump. From equation (6.2) of F99 we obtain [Fe/H] $= -1.8 \pm 0.15$, further supporting our previous estimates.

We obtain also a preliminary estimate of the integrated V magnitude of the cluster, by simple aperture photometry out to $r \simeq 14''$ from the cluster center. This aperture includes the majority of the cluster light but, obviously, since the tenuous cluster halo extends much beyond this limit, the derived integrated luminosity should be considered as a lower limit. We obtain F606W $\simeq 15.5$ mag and F606W $-$ F814W $\simeq 0.8$, which are converted to $V \simeq 15.7$ mag according to equation (1). Correcting for distance and extinction, we find an absolute V magnitude $M_V \lesssim -9.1$, corresponding to a luminosity of $L \gtrsim 3.5 \times 10^5\ L_\odot$.

All the above analysis confirms that B514 is a genuine, very bright, old, and metal-poor globular cluster orbiting at a large distance from the center of M31. The case of B514 demonstrates that the search for remote M31 clusters is a promising line of research that may finally lead to the assembly of a sufficiently large sample of clusters to allow a deeper insight into the yet poorly explored outskirts of our neighbor spiral galaxy.

We acknowledge the financial support to this research by Agenzia Spaziale Italiana (ASI) and the Italian Ministero dell'Università e della Ricerca under grant INAF/PRIN05 1.06.08.03. Part of the data analysis has been carried on with software developed by P. Montegriffo at INAF-Bologna Observatory.

REFERENCES

Bates, S. A., et al. 2004, BAAS, 205, 64.10
Bedin, L. R., Cassisi, S., Castelli, F., Piotto, G., Anderson, J., Salaris, M., Momany, Y., & Pietrinferni, A. 2005, MNRAS, 357, 1038
Bellazzini, M., Ferraro, F. R., & Ibata, R. A. 2003, AJ, 125, 188
Brown, T. M., et al. 2005, AJ, 130, 1693
Bullock, J. S., & Johnston, K. V. 2004, in ASP Conf. Ser. 327, Satellites and Tidal Streams, ed. F. Prada, D. Martinez-Delgado, & T. Mahoney (San Francisco: ASP), 80
Dolphin, A. E. 2000, PASP, 112, 1383
Ferraro, F. R., et al. 1999, AJ, 118, 1738

Galleti, S., Bellazzini, M., Federici, L., & Fusi Pecci, F. 2005, A&A, 436, 535 (G05)
Galleti, S., Federici, L., Bellazzini, M., Buzzoni, A., & Fusi Pecci, F. 2006, A&A, 456, 985
Galleti, S., Federici, L., Bellazzini, M., & Fusi Pecci, F., & Macrina, S. 2004, A&A, 416, 917
Huxor, A.,Tanvir, N. R., Irwin, M. J., Ferguson, A. M. N., Ibata, R. A., Lewis, G. F., & Bridges, T. 2004, in ASP Conf. Ser. 327, Satellites and Tidal Streams, ed. F. Prada, D. Martinez-Delgado, & T. Mahoney (San Francisco: ASP), 118
Ibata, R. A., Irwin, M. J., Lewis, G. F., Ferguson, A. M. N., & Tanvir, N. 2001, Nature, 412, 49
Johnston, K. V., Sigurdsson, S., & Hernquist, L. 1999, MNRAS, 302, 771
McConnachie, A. W., Irwin, M. J., & Ferguson, A. M. N. 2005, MNRAS, 356, 979
Pietrinferni, A., Cassisi, S., Salaris, M., & Castelli, F. 2006, ApJ, 642, 797
Sirianni, M., et al. 2005, PASP, 117, 1049
Stetson, P. 2000, PASP, 112, 925
Zinn, R. 1985, ApJ, 293, 424